Commentary | Open Access

Microstructures

Zhang *et al. Microstructures* **2026**, *6*, 20260120 **DOI:**10.20517/microstructures.2026.151

Reactive ligand confinement for blue perovskite light-emitting diodes

Kun Zhang, Hengyang Xiang, Haibo Zeng

Citation: Zhang, K.; Xiang, H.; Zeng, H. Reactive ligand confinement for blue perovskite light-emitting diodes. *Microstructures* **2026**, *6*, 20260120. https://dx.doi.org/10.20517/microstructures.2026.151

Received: 22 Jun 2026
First Decision: 15 Jul 2026
Revised: 24 Jul 2026
Accepted: 19 Aug 2026
Published: 11 Sep 2026

Academic Editor: Zhigang Chen
Copy Editor: Fangling Lan
Production Editor: Fangling Lan

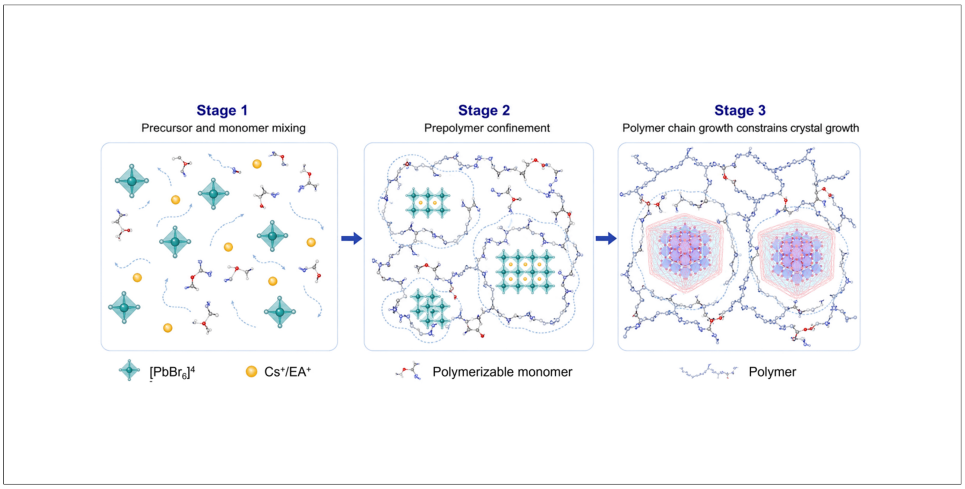

Blue perovskite light-emitting diodes (PeLEDs) remain constrained by the difficulty of combining nanoscale carrier confinement with high crystalline quality. Efficient blue emission also requires low defect density, compositional stability, and balanced charge transport[1-5]. Colloidal nanocrystals enhance radiative recombination through size confinement[6,7], but their assembly into films often produces rough surfaces, discontinuous interparticle contacts, and interfacial defects[8]. Surface ligands can passivate undercoordinated sites, yet dynamic binding and steric bulk may weaken passivation stability and electronic coupling[9,10]. Low-dimensional perovskites provide stronger exciton confinement, but nonuniform quantum well distributions and insulating organic barriers introduce energetic disorder and hinder vertical charge transport[4,5,11].

Liu *et al.*[1] recently reported a nanocrystal confinement strategy based on *in situ* polymerization that addresses the trade-off between grain size and crystalline quality[1]. They introduced oligo (ethylene glycol) methyl ether acrylate (OEGA). Its carbonyl and ether oxygen atoms coordinate with precursor species containing Pb

MIIT Key Laboratory of Advanced Display Materials and Devices, Jiangsu Engineering Research Center for Quantum Dot Display, School of Materials Science and Engineering, Institute of Optoelectronics & Nanomaterials, Nanjing University of Science and Technology, Nanjing 210094, Jiangsu, China.

Correspondence to: Prof. Hengyang Xiang, Prof. Haibo Zeng, MIIT Key Laboratory of Advanced Display Materials and Devices, Jiangsu Engineering Research Center for Quantum Dot Display, School of Materials Science and Engineering, Institute of Optoelectronics & Nanomaterials, Nanjing University of Science and Technology, Nanjing 210094, Jiangsu, China. E-mail: xiang.hengyang@njust.edu.cn; zeng.haibo@njust.edu.cn

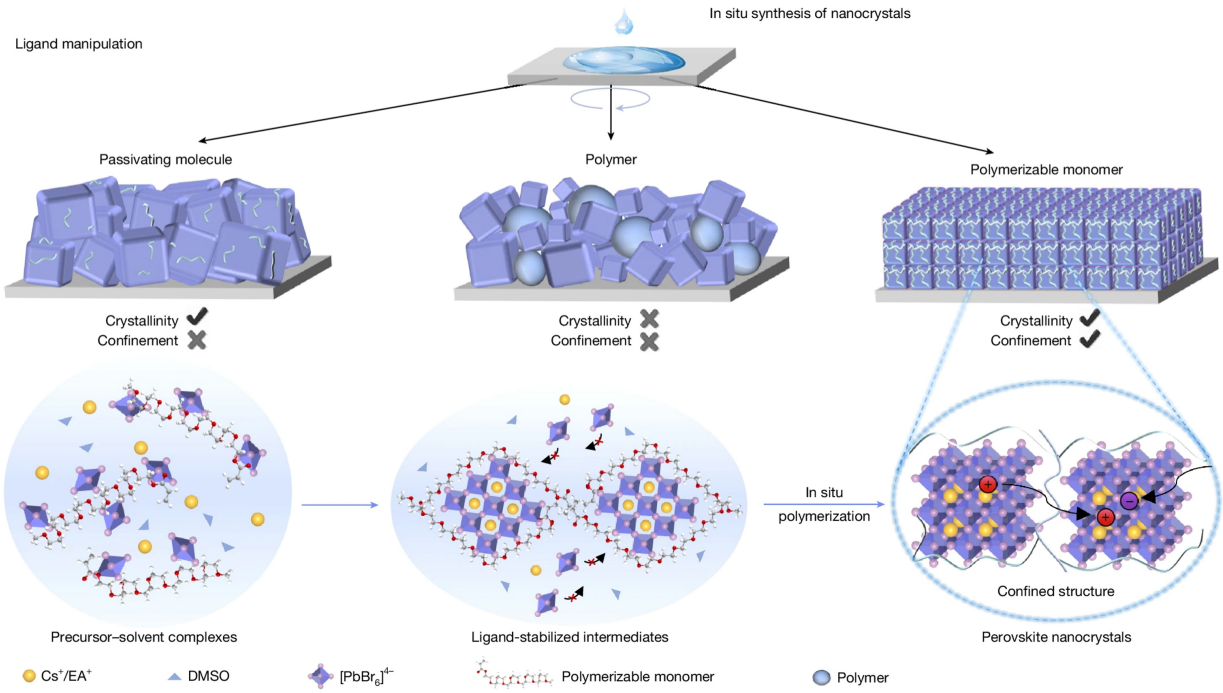

Figure 1. Schematic comparison of passivating molecules, pre-formed polymers and polymerizable monomers in controlling crystallinity and confinement. This figure adapted from Ref.[1], Copyright © 2026 Springer Nature.

and partially displace coordinated dimethyl sulfoxide. During annealing, OEGA polymerizes *in situ* and forms a network around the growing nanocrystals. This sequence slows precursor cluster aggregation, restricts growth at later stages, and allows more time for lattice rearrangement [Figure 1].

This mechanism differs from conventional surface passivation. Small-molecule passivators mainly bind to defects on crystals that have already formed, whereas OEGA participates from the precursor stage and gradually establishes a confining network during growth. The strategy is also distinct from low-dimensional phase engineering. Bulky ammonium cations such as phenethylammonium (PEA^+) and butylammonium (BA^+) divide the three-dimensional $[PbX_6]^{4-}$ framework into inorganic layers of finite thickness[2]. Although this enhances exciton confinement, the organic spacer layers weaken interlayer electronic coupling and vertical charge transport[5]. Earlier polymer approaches were introduced after lattice or heterostructure formation[12,13]. The key advance of Liu *et al.*[1] is that precursor conversion, polymer network formation, and nanocrystal growth occur within the same processing window.

OEGA also modifies the local precursor environment. *In situ* optical measurements show delayed signal onset and slower spectral evolution after OEGA incorporation [Figure 2A]. Liquid-phase electron microscopy further reveals delayed nucleation and stable particles of approximately 10 nm. These observations support slower cluster aggregation, prolonged lattice rearrangement, and restricted growth at later stages, although they do not directly resolve all nonemissive intermediates. Nonpolymerizable small molecules can alter early growth but cannot prevent subsequent grain coarsening. Short chain monomers provide limited coordination and spatial coverage, whereas excessively long chains tend to aggregate and polymerize less efficiently. OEGA therefore offers a favorable balance between coordination and polymerization kinetics.

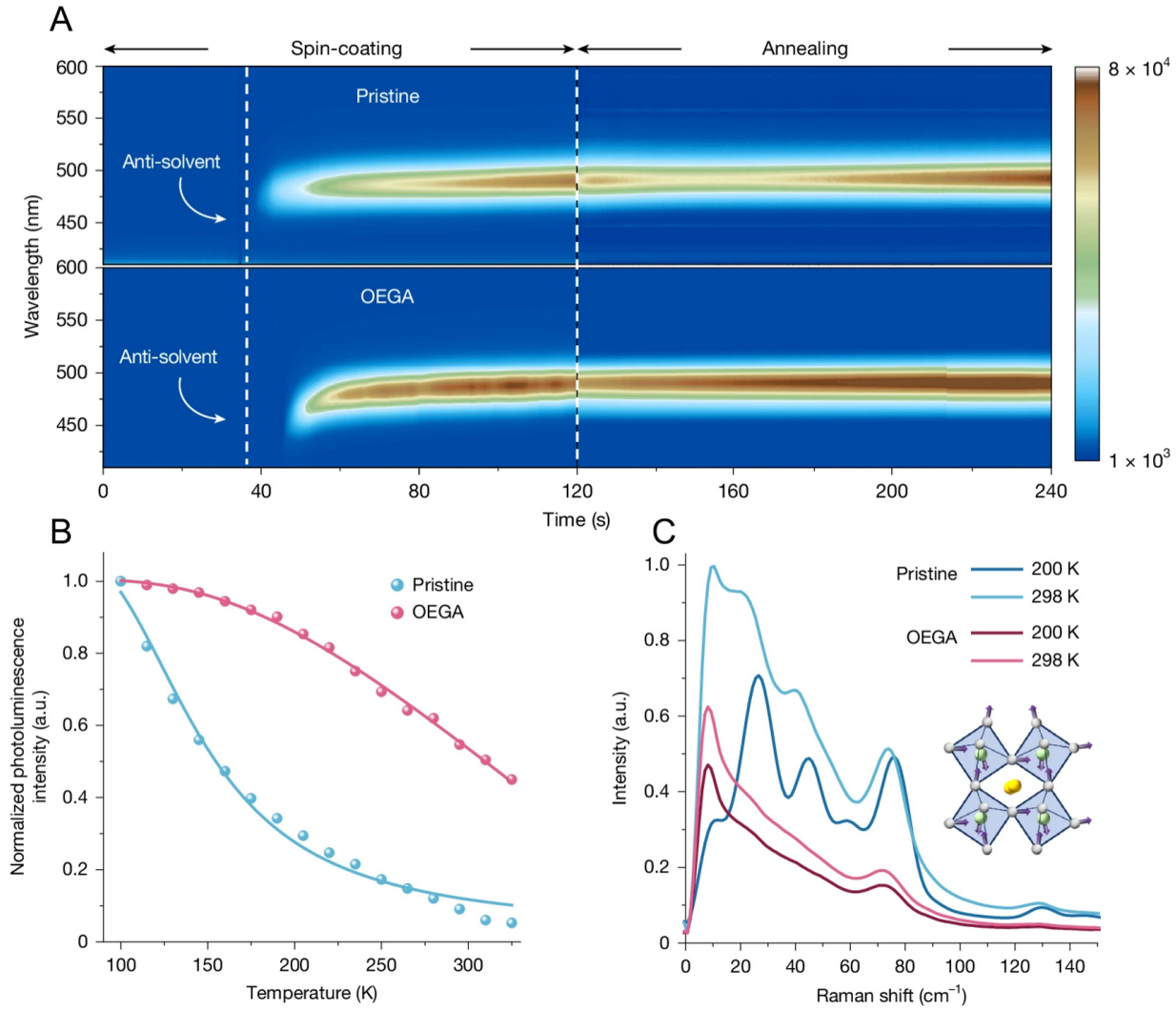

Figure 2. (A) *In situ* photoluminescence evolution of pristine and OEGA-modified perovskite films during spin coating and annealing. (B) Temperature-dependent photoluminescence intensity of pristine and OEGA films. (C) Raman spectra showing reduced lattice vibration features after OEGA treatment. This figure adapted from Ref.[1], Copyright © 2026 Springer Nature.

At the optimized concentration, OEGA confines the nanocrystals to approximately 11 ± 3 nm, and the resulting nanocrystals exhibit cubic symmetry. This phase stabilization is more reasonably attributed to size confinement, surface energy contributions, ethylammonium (EA^+) incorporation, and ligand surface interactions than to selective control of a specific facet. Temperature-dependent photoluminescence shows weaker thermal quenching in OEGA-treated films [Figure 2B]. Spectral linewidth analysis indicates reduced electron-phonon coupling, while low-frequency Raman spectra show weaker lattice vibrational features [Figure 2C]. These results suggest that confinement and lattice relaxation suppress nonradiative recombination[1]. OEGA alone increases the average photoluminescence lifetime from 7.5 to 15.2 ns, and subsequent phenethylammonium bromide (PEABr) treatment extends it to 23.6 ns. PEABr is mainly located at grain boundaries, where they passivate residual defects.

The PeLED adopts an indium tin oxide/modified PEDOT:PSS/perovskite/TPBi/LiF/Al architecture [Figure 3A]. After OEGA and PEABr treatment, it emits at 491 nm with Commission Internationale de l'Eclairage coordinates of (0.07, 0.29) and a full width at half maximum of 23 nm[1]. The peak external quantum efficiency increases from 10.7% to 21.8% [Figure 3B]. At an initial luminance of approximately

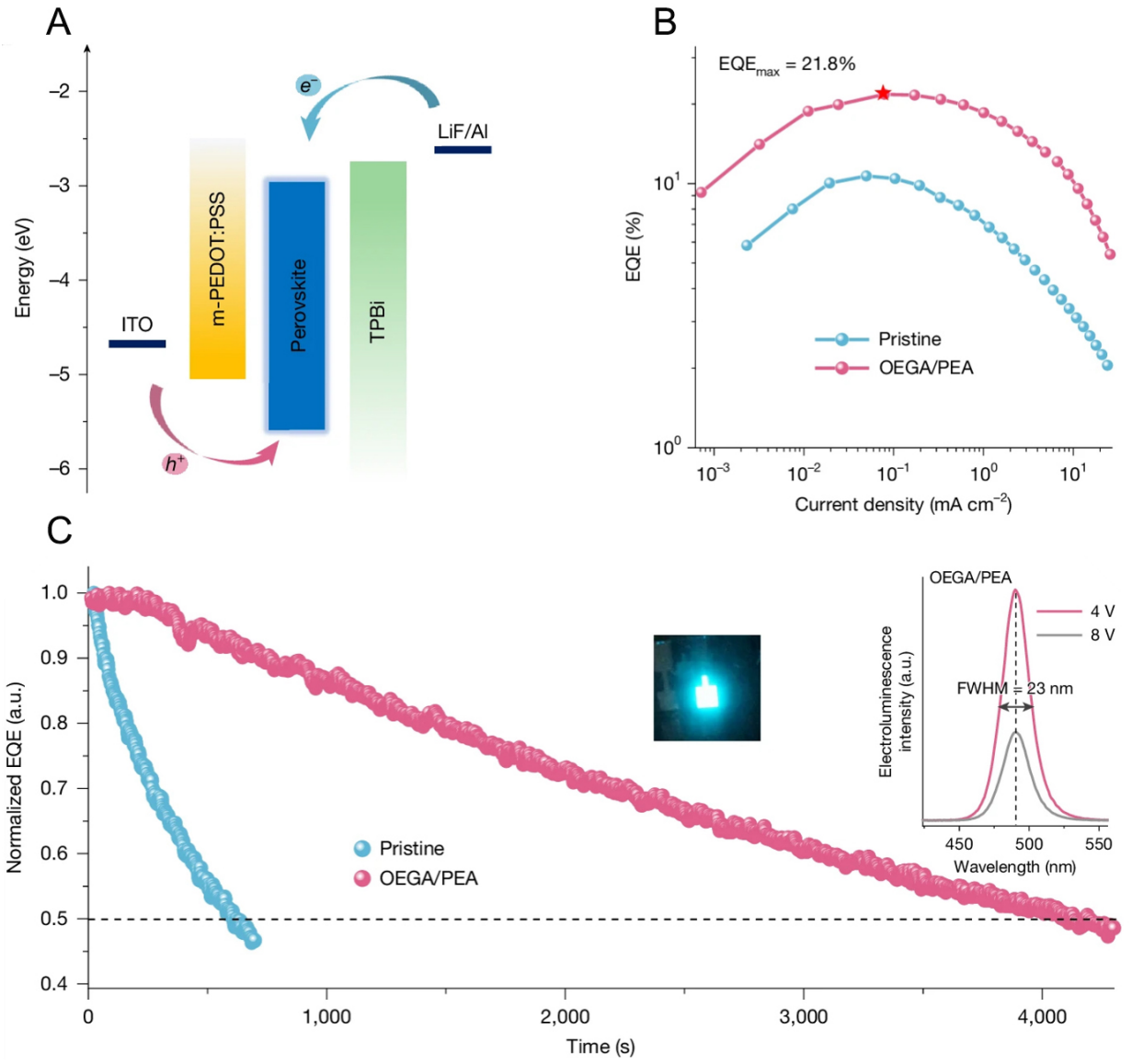

Figure 3. (A) Energy-level diagram of the PeLED structure. (B) External quantum efficiency (EQE)-current density curves of pristine and OEGA/PEA devices. (C) Operational stability and electroluminescence spectra of the OEGA/PEA device. This figure adapted from Ref.[1], Copyright © 2026 Springer Nature.

100 cd m^{-2}, the operational half-lifetime increases from 10.3 to 69.4 min [Figure 3C]. Control devices identify OEGA as the primary contributor, although PEABr-mediated passivation and morphology-related light outcoupling gains also contribute. Temperature-dependent conductivity measurements provide further evidence for enhanced stability. Fitting with a Nernst-Einstein-type relation yields an apparent activation energy for ionic transport of 0.27 eV for the pristine film and 0.77 eV for the OEGA/PEABr treated film[1]. This increase is consistent with more restricted ionic transport. However, the measurement does not identify the dominant mobile species or distinguish among halide migration, A-site cation motion, and interfacial ion accumulation. Time-of-flight secondary ion mass spectrometry combined with operando measurements could help resolve ion redistribution across the device stack.

The strategy was also evaluated in deep-blue devices and sky-blue compositions, formamidinium lead iodide, different substrates, and colloidal nanocrystals. These results suggest that the concept is not restricted to a single composition. However, the most comprehensive device evidence remains limited to an OEGA/PEABr

modified, bromide-rich PeLED emitting at 491 nm. Deep blue mixed-halide devices and chloride-rich devices present more stringent tests because of larger injection barriers and electric field-induced halide segregation[2-5]. Future work should relate ligand structure, coordination strength, chain length, concentration, polymerization kinetics, and network density to nucleation, grain size, phase composition, carrier mobility, ionic conductivity, and device performance. *In situ* grazing incidence wide-angle X-ray scattering could track intermediate formation and phase evolution, while infrared spectroscopy and solid-state nuclear magnetic resonance could clarify polymerization and coordination. Operando ion imaging may reveal ionic transport pathways and interfacial accumulation. Research on lead-free halide light-emitting materials, including $CsCu_2I_3$ and $CsSnI_3$, has advanced rapidly in recent years[14,15]. Reactive ligand confinement offers new opportunities for preparing high-performance lead-free emitters. However, the polymer confinement network must be tailored to the crystallization behavior and charge transport requirements of each material system.

DECLARATIONS

Authors' contributions

Wrote the original draft: Zhang, K.; Xiang, H.
Revised and supervised the project: Xiang, H.; Zeng, H.

Availability of data and materials

Not applicable.

AI and AI-assisted tools statement

During the preparation of this manuscript, the AI tool OpenAI Codex (version GPT-5, released 2025-08-07) was used solely for language editing. The tool did not influence the study design, data collection, analysis, interpretation, or the scientific content of the work. All authors take full responsibility for the accuracy, integrity, and final content of the manuscript.

Financial support and sponsorship

This work was supported by the National Key Research and Development Program of China (No. 2024YFB3612400), the National Natural Science Foundation of China (Nos. 52131304 and U24A20286) and the Natural Science Foundation of Jiangsu Province (BK20240187).

Conflicts of interest

All authors declared that there are no conflicts of interest.

Ethical approval and consent to participate

Not applicable.

Consent for publication

Not applicable.

REFERENCES

1. Liu, S.; Pols, M.; Zhang, Z.; et al. In situ nanocrystal confinement for efficient blue perovskite LEDs. *Nature* **2026**, *654*, 375-82. DOI
2. Liu, X. K.; Xu, W.; Bai, S.; et al. Metal halide perovskites for light-emitting diodes. *Nat. Mater.* **2020**, *20*, 10-21. DOI
3. Jiang, Y.; Qin, C.; Cui, M.; et al. Spectra stable blue perovskite light-emitting diodes. *Nat. Commun.* **2019**, *10*, 1868. DOI PubMed PMC
4. Liu, Y.; Cui, J.; Du, K.; et al. Efficient blue light-emitting diodes based on quantum-confined bromide perovskite nanostructures. *Nat. Photon.* **2019**, *13*, 760-4. DOI
5. Kim, Y. H.; Kim, S.; Kakekhani, A.; et al. Comprehensive defect suppression in perovskite nanocrystals for high-efficiency light-emitting diodes. *Nat. Photon.* **2021**, *15*, 148-55. DOI

6. Xiao, Z.; Kerner, R. A.; Zhao, L.; et al. Efficient perovskite light-emitting diodes featuring nanometre-sized crystallites. *Nat. Photon.* **2017**, *11*, 108-15. DOI
7. Liu, A.; Bi, C.; Li, J.; et al. High color-purity and efficient pure-blue perovskite light-emitting diodes based on strongly confined monodispersed quantum dots. *Nano. Lett.* **2023**, *23*, 2405-11. DOI
8. Shamsi, J.; Rainò, G.; Kovalenko, M. V.; Stranks, S. D. To nano or not to nano for bright halide perovskite emitters. *Nat. Nanotechnol.* **2021**, *16*, 1164-8. DOI PubMed
9. Yuan, S.; Dai, L.; Sun, Y.; et al. Efficient blue electroluminescence from reduced-dimensional perovskites. *Nat. Photon.* **2024**, *18*, 425-31. DOI
10. Ma, D.; Lin, K.; Dong, Y.; et al. Distribution control enables efficient reduced-dimensional perovskite LEDs. *Nature* **2021**, *599*, 594-8. DOI
11. Fiuza-Maneiro, N.; Sun, K.; López-Fernández, I.; Gómez-Graña, S.; Müller-Buschbaum, P.; Polavarapu, L. Ligand chemistry of inorganic lead halide perovskite nanocrystals. *ACS. Energy. Lett.* **2023**, *8*, 1152-91. DOI
12. Chen, W.; Shi, Y.; Chen, J.; et al. Polymerized hybrid perovskites with enhanced stability, flexibility, and lattice rigidity. *Adv. Mater.* **2021**, *33*, 2104842. DOI
13. Proppe, A. H.; Wei, M.; Chen, B.; Quintero-Bermudez, R.; Kelley, S. O.; Sargent, E. H. Photochemically cross-linked quantum well ligands for 2D/3D perovskite photovoltaics with improved photovoltage and stability. *J. Am. Chem. Soc.* **2019**, *141*, 14180-9. DOI
14. Shen, Y.; Meng, K.; Zhao, Y.; et al. Lead-free halide perovskites for efficient light-emitting devices. *FlexMat* **2026**, *1*, 1-41. DOI
15. Guo, H.; Shi, L.; Shi, Z.; He, Y.; Zhu, Y. Direct synthesis of high quantum yield lead-free $CsCu_2I_3$ powder in water and its application in yellow LED. *Exploration* **2024**, *5*, 20240004. DOI PubMed PMC